HHS Public Access

Author manuscript

Contrast Media Mol Imaging. Author manuscript; available in PMC 2021 August 16.

Published in final edited form as:

Contrast Media Mol Imaging. 2011 ; 6(3): 148–152. doi:10.1002/cmmi.409.

Optimizing quantitative *in vivo* fluorescence imaging with near-infrared quantum dots

Lauren T. Rosenblum[a], **Nobuyuki Kosaka**[a], **Makoto Mitsunaga**[a], **Peter L. Choyke**[a], **Hisataka Kobayashi**[a,*]

[a]Kobayashi Molecular Imaging Program, Center for Cancer Research, National Cancer Institute, National Institutes of Health, 10 Center Dr., Bethesda, MD 20892-1088, USA

Abstract

Quantum dots (QDs) are fluorescent nanoparticles with broad excitation and narrow, wavelength-tunable emission spectra. They are used extensively for *in vitro* fluorescence imaging studies and more recently for *in vivo* small animal and pre-clinical studies. To date there has been little concern about the selection of QD size (and thus emission wavelength peak) and excitation wavelengths, as they have little relevance to the results of *in vitro* studies. *In vivo* imaging, however, poses additional constraints, such as the scattering and absorption by tissue, which may influence the signal intensity at the body surface. Here, we demonstrate that longer-wavelength excitation and emission yield less quantization error in measured relative fluorescence intensity, using three near-infrared QDs (QD655, QD705 and QD800) applied to *in vivo* lymphatic imaging, and a range of excitation wavelengths from the blue to the red. Statistically significant differences in quantization error were observed between nearly all pairs of excitation wavelengths (445–490, 503–555, 575–605, 615–665 and 671–705 nm). Similarly, quantization error decreased with longer emission wavelengths (655, 705 and 800 nm). Light absorbance and scattering were demonstrated to be more potent factors than absorbance efficiency of QDs in producing quantization error in the measured fluorescence intensity. As a result, while wavelengths can be adjusted for qualitative experiments, the longest possible wave-lengths should be used if quantification is desired during QD imaging experiments.

Keywords

fluorescence imaging; *in vivo* imaging; quantum dot; quantitative imaging; nanotechnology

1. Introduction

Fluorescence imaging is a rapidly growing field owing to its several advantages, including portability, lack of ionizing radiation, lower expense, higher sensitivity, multi-color capabilities and the switchable nature of some optical probes (1). Disadvantages (related to the individual fluorescence probe) include instability, poor penetration of light through tissue, autofluorescence and difficulties in quantification. However, the broad range of

*Correspondence to: H. Kobayashi, Molecular Imaging Program, Center for Cancer Research, National Cancer Institute, National Institutes of Health, Building 10, Room B3B69, 10 Center Dr., Bethesda, MD 20892-1088, USA. kobayash@mail.nih.gov.

available fluorophores allows considerable latitude in the selection of optimized photonics. Whereas organic fluorophores and fluorescent proteins are relatively unstable, in contrast, quantum dots (QDs) have minimal photo- and biological degradation (2,3). Moreover, QDs are very bright and therefore penetrate deeper into tissue and, due to their narrow emission peaks, multiple QDs can be employed simultaneously. While questions remain about the suitability of QDs for human use, they are often used in animal studies and a literature describing their use has been developed (3,4).

The emission peak of a QD depends on the bandgap energy which in turn depends on the size of the QD (5,6). As a result, both the wavelengths of excitation and emission vary considerably (3). To date there has been little concern about the selection of particular QDs for particular applications since the *in vitro* behavior of QDs indicates a broad range for excitation wavelength and high efficiency for emission. However, in vivo imaging poses additional constraints. For instance, the scattering and absorption of tissue may influence the signal intensity at the body surface. In general, the absorbance efficiency of QDs decreases with increasing wavelength of both excitation and emission (which can be adjusted with the size of the QDs), yielding weaker emissions (7). However, this factor could be balanced or overcome by better tissue penetration of longer wavelength light. In addition, the greater the gap between the excitation wavelength and the emission peak wavelength, the less interference there will be from autofluorescence (2). In contrast, scatter and absorbance by endogenous tissue also decrease with increasing wavelength.

It is often assumed that emissions in the near-infrared (NIR) are less susceptible to these limitations and that the excitation wavelength and QD can be chosen at will. Here, we evaluate the quantitative capabilities of fluorescence lymphatic imaging using three NIR QDs to establish the optimal optical settings for quantitative fluorescence imaging *in vivo*.

2. Experimental section

2.1. Chemicals/reagents

Carboxyl quantum dots, QDot® 655 ITK™ (peak emission wavelength 655 nm), QDot® 705 ITK™ (peak emission wave length 705 nm), and QDot® 800 ITK™ (peak emission wavelength 800 nm) were purchased from Invitrogen Corporation (Eugene, OR, USA; Fig. 1). QDs had a CdTe core with a thin semi-conductor shell of ZnS. Quantum dots were diluted in PBS to working concentrations of 0.8 μM (for QD655 and QD705) and 2.0 μM (for QD800, due to decreased fluorescence intensity). Sodium pentobarbital (5 mg ml^{-1} in PBS) was purchased from Ovation Pharmaceuticals Inc. (Deerfield, IL).

2.2. Procedure

All *in vivo* procedures were carried out in compliance with the Guide for the Care and Use of Laboratory Animal Resources (1996), National Research Council, and approved by the National Cancer Institute Animal Care and Use Committee. Female athymic mice (nu/nu) were anesthetized with intraperitoneal injections of up to 250 μl sodium pentobarbital (5 mg ml^{-1}). Each mouse was given five consecutive intracutaneous injections of 10 μl QD655, QD705 or QD800 into each upper extremity, each ear and the lower lip. Mice were then

positioned in the supine position with non-fluorescent tape, which was also used to cover the sites of injection to prevent image artifacts.

Spectral fluorescence images were taken with Maestro In-Vivo Imaging System (CRI Inc., Worburn, MA, USA) using a tunable filter which was stepped in 10 nm increments from 600 to 900 nm. Images were obtained with five excitation-emission filter sets: blue (excitation 445–490 nm, emission 645 nm longpass), green (excitation 503–555 nm, emission 645 nm longpass), yellow (excitation 575–605 nm, emission 645 nm longpass), red (excitation 615–665 nm, emission 700 nm longpass) and deep red (excitation 671–705 nm, emission 750 nm longpass; Fig. 2b, e).

Following *in vivo* spectral imaging, mice were euthanized by carbon dioxide inhalation. The fluorescent lymph nodes (superficial cervical, deep cervical, brachial and axillary lymph nodes) were then resected and *ex vivo* spectral fluorescence images, to be used as standards, were acquired using the green filter set (Fig. 2a, d). Resected lymph nodes were then covered with a flap of skin (approximately 0.5 mm thick) and spectral fluorescence images were acquired using the same filter sets as for the *in vivo* images (Fig. 2c, f).

2.3. Analysis

All collected images were unmixed and analyzed using the Maestro software, which uses spectra unmixing algorithms to separate QD signals and autofluorescence signal (whose spectra were acquired separately with QD solutions and a control mouse). Only the unmixed image of the QD fluorescence was analyzed.

The average fluorescence intensity above a consistent threshold value was determined for each lymph node in the *ex vivo* images. For each mouse, average fluorescence intensity was determined for the regions around each lymph node, which were drawn in the image acquired with the longest-wavelength filter set in the *in vivo* and covered *ex vivo* experiments. A minimum of 32 fluorescent lymph nodes were analyzed for each QD.

A standard lymph node was defined as the brightest node on each *ex vivo* image. To eliminate differences due to injections and lymph node uptakes, relative fluorescence intensities were calculated with respect to that standard lymph node for all *ex vivo* standard (S), *in vivo* (I) and covered *ex vivo* (C) nodes. Ideally, the relative intensities for the lymph nodes of each mouse would be identical for the S, I, and C nodes, although *in vivo* quantization error-inducing factors prevent this. The relative quantization error of the fluorescence intensity of each lymph node in the *in vivo* and skin-covered *ex vivo* images, relative to the *ex vivo* standards, was calculated using the following formula: relative quantization error = $|(S - I)/S|$ or = $|(S - C)/S|$, for the *in vivo* and covered *exI vivo* images, respectively.

Mean relative quantization errors with the different filter sets for each QD were compared with a repeated measures ANOVA statistical analysis with the Tukey post test, using GraphPad Instat statistical software (version 3.06 and GraphPad Prism, GraphPad Software, La Jolla, CA, USA). Values of $p < 0.05$ were considered statistically significant. Additionally, pairs of filter sets were compared by Wilcoxon matched-pairs signed rank

tests, a non-parametric test which ranks the absolute values of the differences between data pairs, sums the ranks (which have been assigned a sign based on which value in the pair was greater), and uses the rank sum to determine statistical significance (8). Values of $p < 0.05$ were considered statistically significant.

3. Results

3.1. Fluorescence intensity quantization error trends *in vivo*

Quantization errors for each excitation emission also decreased or remained constant with increasing emission wavelength of emission, although no statistically significant differences were evident. Error differences between all pairs of filter sets with the exception of the deep red and red with QD800, and the green and blue with QD655 were statistically significant according to the Wilcoxon test. Also, while differences in mean quantization errors for different filter settings were only statistically significant by the repeated measures ANOVA in most cases, a general trend of increasing error with decreasing excitation wavelength was observed, similar to the trend for the majority of individual lymph nodes. For the shortest wavelength QD, QD655, yellow excitation demonstrated less statistically significant relative error in fluorescence intensity of *in vivo* images over both green and blue excitation ($p < 0.01$). Similarly, for QD705, there was statistically significantly less error with red excitation than with both green and blue excitation ($p < 0.05$) and a trend of increasing error with decreasing wavelength can be clearly seen. Lastly, along with a similar trend in relative quantization error, blue excitation produced more relative intensity quantization error than both red ($p < 0.05$) and deep red ($p < 0.01$) excitation for QD800 (Fig. 3). Overall, it was demonstrated that longer-wavelength light results in less relative quantization error for *in vivo* imaging of QDs of various emission wavelengths.

3.2. Minimal fluorescence intensity quantization error *ex vivo* with skin covering

No statistical difference was demonstrated by the repeated measures ANOVA in the relative fluorescence intensity of lymph nodes ($n = 30$) between excitation wavelengths for QD655. As the excitation wavelength was increased, the standard quantization error of the measurement decreased slightly: blue filter (mean = 0.236; standard error = 0.037), green filter (0.221; 0.033), yellow filter (0.217; 0.029). Similarly, no statistically significant differences were seen with different excitation wavelengths for QD705 ($n = 21$). A similar trend in standard error was seen with increasing excitation wavelength: blue (0.189; 0.037), green (0.185; 0.032), yellow (0.167; 0.031) and red (0.165; 0.029). Finally, no statistically significant differences were seen between filter sets with QD800 ($n = 32$). In this case, no trend was observed, with varying errors for the filters of blue (0.356; 0.037), green (0.287; 0.029), yellow (0.266; 0.023), red (0.297; 0.028) and deep red (0.297; 0.030) (Fig. 4). The Wilcoxon analysis reported a few scattered significant differences between the red and blue, the yellow and blue, and the green and blue sets for QD800, and the yellow and green sets for QD705.

4. Discussion

QDs have become popular for pre-clinical fluorescence imaging due to numerous advantages over conventional fluorophores, particularly increased brightness, wavelength flexibility and stability (3). QD fluorescence imaging *in vivo* has been extensively studied for molecular, cellular, and lymphatic imaging as well as pre-clinical studies (9–12). Because of these qualities and the potential for multi-color imaging, QDs are good candidates for the specific imaging of cancer, both with live cell tracking and *in vivo* targeted imaging (6). Nanoparticle-mediated drug delivery could particularly benefit from improvement of imaging with more quantitative biodistribution and pharmacokinetic data (13).

Despite their photo-physical advantages, QDs also have limitations. Upon intravenous injection, their relatively large size leads to increased circulation times and possible non-specific uptake by the reticulo-endothelial system. Their composition, consisting primarily of two or three heavy metals, leads to concern over toxicity *in vivo* (4,14). Topological application of QDs, such as for lymphatic imaging shown in this study, can minimize the administration dose. Thus, this represents a very feasible application for the clinical practice, though further toxicity testing should be done.

However, such uses depend on accurate quantification. As the field of optical imaging with QDs continues to grow, questions regarding the ability to quantify results become increasingly important. QDs absorb over a broad range of light, with absorption efficiency sharply increasing towards the UV-blue range (Fig. 1). For example, extinction coefficients at 532 nm excitation (QD655 and QD705 at 2 100 000 cm^{-1} M^{-1}; QD800 at 2 000 000 cm^{-1} M^{-1}) are significantly lower than those at 350 nm (9 100 000 cm^{-1} M^{-1} for QD655; 12 900 000 cm^{-1} M^{-1} for QD705; and 12 600 000 cm^{-1} M^{-1} for QD800) (7). As a result, excitation with bluer light results in stronger QD fluorescence signal *in vitro*. Therefore, blue-violet excitation is the common optical setting for observing cells under a fluorescence microscope.

Other factors are at play, however, for *in vivo* imaging. Shorter wavelength excitation enables a larger gap between the excitation wavelength and the emission peak of the QD, which minimizes autofluorescence, which occurs near the excitation wavelength. Fluorescence signal can be decreased however with bluer (shorter) wavelengths due to increased attenuation of the incident light. More specifically, two factors might contribute to an increase in error with shorter wavelength excitation during *in vivo* imaging: increased absorbance by endogenous tissue and increased scattering by small molecules. Over the range of QDs and excitation wavelengths studied, there is a fairly steady decrease in light absorbance by endogenous tissue, with the least absorption in the ‘optical window’ of 650–900 nm (1,15). Additionally, the intensity of scattered light is inversely proportional to the wavelength of the light to the fourth power, so that scattering increases dramatically with decreasing wavelength. The interplay of the increased absorbance efficiency and decreased incident light for bluer wavelengths on the error of measured fluorescence intensity for *in vivo* experiments is of relevance to the selection of QDs.

What wavelength of light should be used to excite QDs for *in vivo* experiments for minimal error in quantitative fluorescence measurements? The quantization error in fluorescence intensity was compared for three different QDs and for excitation light of five different wavelengths. Light absorbance and scattering were demonstrated to be more potent factors than absorbance efficiency of QDs in producing error in the measured fluorescence intensity. It was found that the longer (more red) wavelengths were, in fact, best for quantitative imaging with all studied QDs.

Quantization errors in relative fluorescence intensity were found to decrease with longer wavelengths of both excitation (with statistical significance) and emission. Quantization error differences between all pairs of filter sets, with the exception of the deep red and red with QD800, and the green and blue with QD655 (also the only pair that had an apparent increase in error with an increase in wavelength), were statistically significant. Quantization errors for each excitation filter also decreased or remained constant with increasing wavelength of emission (as determined by comparing errors with different QDs), although no statistically significant differences were evident. In this study, we used spectrally resolved imaging to eliminate background autofluorescence and extract the QD signal, largely eliminating autofluorescence. Although both extinction coefficient and quantum yield of shorter excitation wavelengths were the largest, the smallest error value was found with QD800 and the deep red excitation filter set, suggesting that longer wavelength excitation and emission should be used.

Differences in quantization error might be attributable to differences in the filter sets, particularly differences in the bandpass width of the excitation filter. The skin-covered *ex vivo* experiment, however, provides evidence that experimental set-up is not the cause of error differences. In this experiment, minimal error was measured for each of the filter sets, and there were no statistically significant differences between them according to the repeated measures ANOVA. There were only a few statistically significant pairings, all but one involving the blue filter set for QD800. While relative fluorescence errors for the in vivo experiments ranged from 0.83 to 2.69, errors in the skin-covering experiment were relatively minimal (ranging from 0.17 to 0.36). Additionally, the errors between the QDs (with different emission peaks) and those for QD800 did not progress in the same pattern as the error for the *in vivo* experiment (increasing with decreasing wavelength). This suggests that the most substantial errors are introduced by the depth of the enhancing tissue structures and are not merely related to differences in filter sets.

The ability to select wavelengths of excitation and emission for QD-based experiments contributes to the attractiveness of QDs. While this capability is useful, care must be exercised in the choice of excitation and emission wavelengths or substantial errors in quantification can occur in the *in vivo* setting. As we have shown, error in relative fluorescence measurement, that is, the difference in signal between the *ex vivo* and *in vivo* setting, is lessened through the use of longer wavelengths of both excitation and emission. While wavelengths can be adjusted for qualitative experiments, the longest possible wavelengths should be used if quantification is desired during QD imaging experiments.

Acknowledgements

This research was supported by the Intramural Research Program of the NIH, National Cancer Institute, Center for Cancer Research.

REFERENCES

1. Weissleder RA clearer vision for in vivo imaging. Nat Biotechnol2001; 19: 316–317. [PubMed: 11283581]
2. Kobayashi H, Koyama Y, Barrett T, Hama Y, Regino CAS, Shin IS, Jang BS, Le N, Paik CH, Choyke PL, Urano Y. Multimodal nanop-robes for radionuclide and five-color near-infrared optical lymphatic imaging. ACS Nano2007; 1: 258–264. [PubMed: 19079788]
3. Smith AM, Duan HW, Mohs AM, Nie SM. Bioconjugated quantum dots for in vivo molecular and cellular imaging. Adv Drug Deliv Rev2008; 60: 61226–1240.
4. Jamieson T, Bakhshi R, Petrova D, Pocock R, Imani M, Seifalian AM. Biological applications of quantum dots. Biomaterials. 2007; 28: 4717–4732. [PubMed: 17686516]
5. Efros AL. Interband absorption of light in a semiconductor sphere. Soviet Phys Semiconductors-USSR1982; 16: 772–775.
6. Smith AM, Dave S, Nie SM, True L, Gao XH. Multicolor quantum dots for molecular diagnostics of cancer. Exp Rev Mol Diagn2006; 6: 231–244.
7. Qdot® ITKTM Carboxyl Quantum Dots. Probes IM, Molecular Probes/Invitrogen Website: http://probes.invitrogen.com/media/pis/mp19020.pdf (accessed 20 December 2007).
8. Wilcoxon FIndividual comparisons by ranking methods. Biometr Bull1945; 1: 80–83.
9. Medintz IL, Uyeda HT, Goldman ER, Mattoussi H. Quantum dot bioconjugates for imaging, labelling and sensing. Nat Mater2005; 4: 435–446. [PubMed: 15928695]
10. Kosaka N, Ogawa M, Sato N, Choyke PL, Kobayashi H. In vivo real-time, multicolor, quantum dot lymphatic imaging. J Invest Dermatol2009; 129: 2818–2822. [PubMed: 19536144]
11. Kosaka N, Ogawa M, Choyke PL, Kobayashi H. Clinical implications of near-infrared fluorescence imaging in cancer. Future Oncol2009; 5: 1501–1511. [PubMed: 19903075]
12. Medintz IL, Mattoussi H, Clapp AR. Potential clinical applications of quantum dots. Int J Nanomed2008; 3: 151–167.
13. Delehanty JB, Boeneman K, Bradburne CE, Robertson K, Medintz IL. Quantum dots: a powerful tool for understanding the intricacies of nanoparticle-mediated drug delivery. Exp Opin Drug Deliv2009; 6: 1091–1112.
14. Rzigalinski BA, Strobl JS. Cadmium-containing nanoparticles: perspectives on pharmacology and toxicology of quantum dots. Toxicol Appl Pharm2009; 238: 280–288.
15. Konig KMultiphoton microscopy in life sciences. J Microsc (Oxford)2000; 200: 83–104. [PubMed: 11106949]

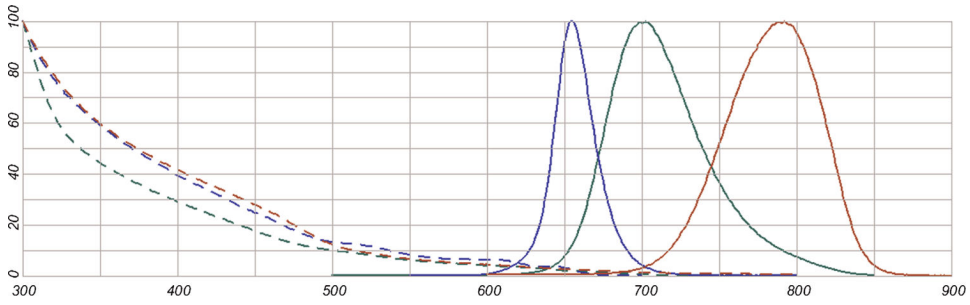

Figure 1.

Absorbance spectra (dashed lines) and emission spectra (solid lines) for QD655 (blue), QD705 (green) and QD800 (red).

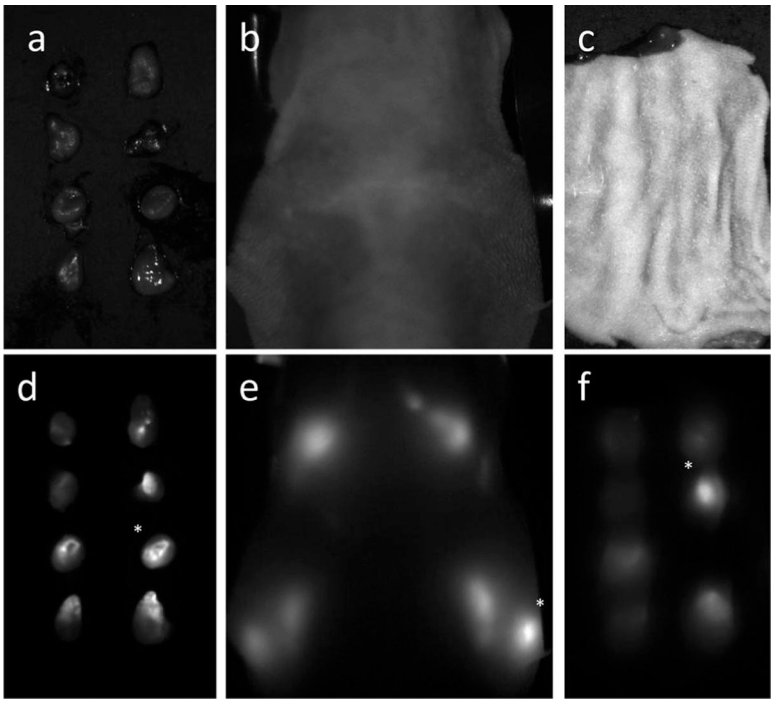

Figure 2.

Relative fluorescence intensities of the lymph nodes in each image [*ex vivo* (a, d; white light and fluorescence images), *in vivo* with deep red (b, e), red, yellow, green and blue excitation, *ex vivo* with skin covering with deep red (c, f), red, yellow, green and blue excitation] were calculated relative to the standard node, which was set as the brightest node for each mouse in the *ex vivo* image. The *ex vivo* relative intensities (S_n) were used as the gold standards and the quantization error (En) in fluorescence intensity (I_n) was calculated relative to those intensities ($E_n = |(S_n - I_n)/S_n|$ for each n, or lymph node).

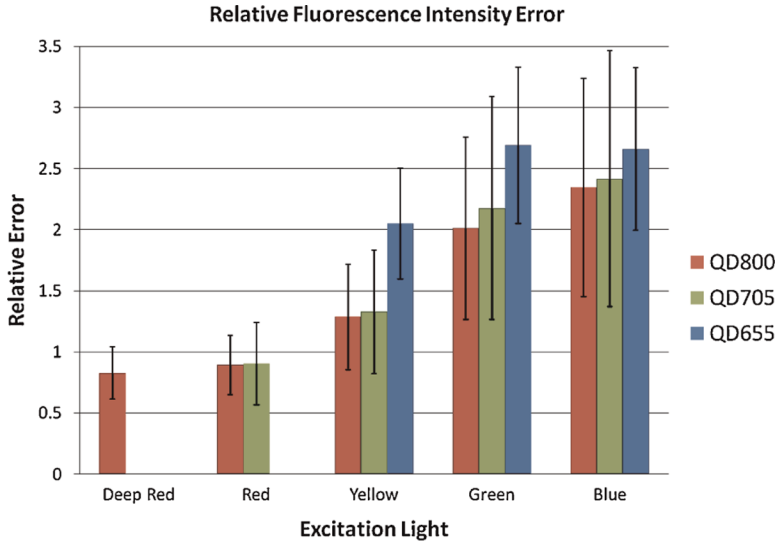

Figure 3.

Relative fluorescence intensity quantization error for *in vivo* lymph nodes relative to *ex vivo* standards, at different excitation wavelengths for QD800 (red), QD705 (green) and QD655 (blue).

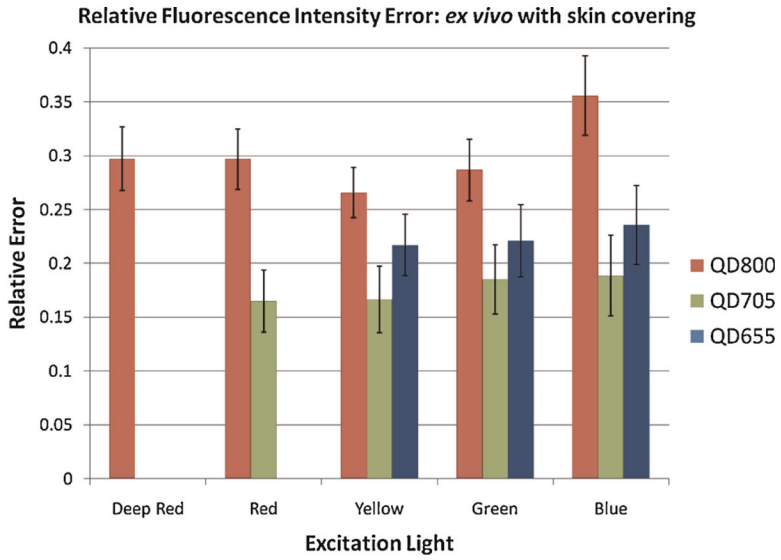

Figure 4.

Relative fluorescence intensity quantization error for *ex vivo* lymph nodes with skin covering relative to *ex vivo* standards, at different excitation wavelengths for QD800 (red), QD705 (green) and QD655 (blue).